Effect of the Range of Interactions on the Properties of Fluids. 2. Structure and Phase Behavior of Acetonitrile, Hydrogen Fluoride, and Formic Acid

Ariel A. Chialvo,*,† Matthias Kettler,‡ and Ivo Nezbeda§,||

Chemical Sciences Division, Aqueous Chemistry and Geochemistry Group, Oak Ridge National Laboratory, Oak Ridge, Tennessee 37831-6110, Institute of Theoretical Physics, Computer Simulation Group, University of Leipzig, Leipzig, Germany, E. Hála Laboratory of Thermodynamics, Academy of Sciences, 165 02 Prague 6, Czech Republic, and Department of Physics, Purkyně University, 400 96 Ústí Lab., Czech Republic

Received: February 22, 2005; In Final Form: March 11, 2005

To complete the study on the effect of the long-range part of Coulombic interactions on properties of complex polar and associating fluids, we have investigated in detail three compounds with extreme features: acetonitrile for its unusually large dipole moment, hydrogen fluoride with very strong hydrogen bonding, and formic acid for its potential formation of different *n*-mers in liquid and gaseous phases. The effect of the long-range Coulombic interactions on both the structure and thermodynamics of the homogeneous phase, and on the vapor−liquid equilibria has been examined using the same decomposition of realistic potential models into a short-range part and a residual part as in the previous paper [Kettler, M.; et al. *J. Phys. Chem. B* **2002**, *106*, 7537−7546]. The present results fully confirm the previous findings that the properties of polar and associating systems are determined primarily by the short-range interactions regardless of their nature, i.e., contributions arising from the long-range interactions constitute only a small portion of the total properties, and thus that the short-range potential counterpart of full realistic models can be used as a convenient reference for a successful perturbation expansion.

1. Introduction

A challenging aspect in the development of accurate molecular-based equation of state for real fluids is the adequate formulation of simple configurational Hamiltonians able to account properly for the underlying intermolecular forces and, simultaneously, to give a tractable mathematical form amenable to engineering calculations. The traditional engineering approach to tackle this task has been through the use of an idealized model Hamiltonian (or the Helmholtz free energy counterpart), such as the ideal gas, as a reference to which the contributions of relevant interactions, short-range (dispersion), specific (hydrogen bond), and long-range (multipole expansion of electrostatics) are added.[1,2] This approach is equivalent to a mapping of the residual properties of a fluid to particular types of intermolecular forces, through regression of experimental data. For the particular case of associating and polar fluids, their thermodynamic behavior has been attributed to the presence of long-range electrostatic interactions and, consequently, their modeling has always included these interactions as dominant contributions.[3]

However, recent work by this group (for a review see ref 4 and references therein) has challenged such a concept by suggesting that the range (or equivalently, the rate of decay with increasing intermolecular distance) rather than the type of interactions is the main factor responsible for dictating the thermophysical behavior of fluids. This suggestion has then been supported by systematic molecular simulation studies of the effect of the interaction range on the thermodynamic and structural properties of homogeneous phases, as well as the vapor−liquid equilibria (including critical conditions) of realistic model fluids, including water, methanol, acetone, and carbon dioxide.[5−8] To be more specific, our simulation results have shown unambiguously that the long-range portion of the electrostatic interactions accounts only for a few percent of the corresponding total configurational internal energy, affects, to a certain extent, the shape of the dipole−dipole pair distribution functions while preserving some related integrals (e.g., dielectric permittivity), and has negligible effect on the site−site correlation functions.

These findings have profound modeling implications, beyond their obvious theoretical significance; that is, they identify the short-range part of the Hamiltonians as the natural and convenient reference for the development of fast converging perturbation expansions such that the contributions of the long-range interactions to any thermophysical property can be simply treated as a perturbation. It is worth recalling that the rationale behind the range of the intermolecular interactions was also the foundation of earlier successful perturbation theories for simple, i.e., argon-like, fluids, such as the Barker−Henderson[9] or WCA[10] theories for soft-sphere fluids, where the short range is given by the repulsive part of the Lennard-Jones potential and the attractive Lennard-Jones tail (i.e., the long-range part of the full potential) is treated as a perturbation.

Obviously, there is a persisting interest in finding possible limitations of the proposed intermolecular potential split as a way to extend the concomitant perturbation approach to increasingly complex fluids and their mixtures, toward the ultimate goals of developing true molecular-based equations of state.[11,12] From the practical viewpoint, the quest for those limitations should be pursued by studying representative fluids

* To whom correspondence should be addressed. E-mail: chialvoaa@ornl.gov.
† Oak Ridge National Laboratory.
‡ University of Leipzig.
§ Academy of Sciences.
|| Purkyně University.

10.1021/jp050922u CCC: $30.25
Published on Web 04/14/2005

from the hierarchy of increasing complexity, e.g., from normal (uncharged and apolar) to polar, and then to associating fluids (i.e., systems incorporating, in addition, strong long-range electrostatic interactions, strong and strongly orientation-dependent short-range attractive interactions),[1] so that in the process we would find answers to the following questions: Are the findings on the short-range modeling of thermophysical, structural, and vapor−liquid equilibrium (VLE) properties still valid for (a) molecular systems with increasingly larger dipole moments and (b) molecular systems exhibiting increasingly stronger association?

Therefore, the goal of this work is to extend our previous analysis[8] to three specific fluids: formic acid, hydrogen fluoride, and acetonitrile, which are characterized by the increasing strength of their dipole moment, i.e., from 1.4 to 4.1 D (Appendix D-3 in ref 3). These three fluids share the same property of being dipolar, though the first two are protic and the last is aprotic. In other words, formic acid and hydrogen fluoride are able to form hydrogen bond (HB) structures and dissociate as Bronsted acids, in contrast to acetonitrile that, despite its large dipole moment, does not associate.

On one hand, carboxylic acids (e.g., formic acid) are known to form relatively strong hydrogen bonds. However, unlike alcohols, they tend to form dimers (primarily in the gaseous phase) rather than polymeric chain aggregates, and the degree of their association rapidly decreases with rising temperature to predominantly monomeric molecules.

On the other hand, as a hydracid HF shares some remarkable similarities with water in that they are isoelectronics. In particular, HF's dipole moment is 1.4 D and its normal dielectric constant is about 83, compared to 1.85 D and 78 for normal water. Therefore, even though HF has only one hydrogen (as opposed to two in water) to promote association, its linear geometry promotes chained hydrogen bonding structures in contrast to water's three-dimensional hydrogen bonding structures.

Moreover, formic acid and methanol share similar properties, including HB-association, though formic acid also dissociates. Methanol has a dipole moment of about 1.7 D and a dielectric permittivity of about 33, in comparison to, respectively, about 1.4 D and 58 for formic acid (in principle, the acid and its corresponding alcohol have similar dipole moments but lower dielectric constants due to the canceling of the dipole−dipole interaction during association).

Finally, acetonitrile neither associates nor dissociates, though its large dipole moment and linear geometry make it an ideal candidate as the dipolar counterpart of carbon dioxide (i.e., a linear molecule with a large quadrupole moment).

The present analysis of these three distinctive fluids becomes the required first step in the pursuit of successful perturbation expansions about suitable references, in that it provides the theoretical support to the split of the intermolecular potentials into short- and long-range contributions, which is the basis for our recently proposed[13−16] fundamental approach to the development of primitive counterparts of realistic intermolecular potentials.

This paper is organized as follows. In section 2 we introduce the intermolecular potential models used in this study, summarize the main features of the short-range formalism, and provide some relevant information on the simulation methodology. In section 3, we first discuss the molecular dynamics results for the thermophysical and structural properties of homogeneous phases along one liquid density isochore and one supercritical isotherm, and then interpret the finding on the comparison of the VLE behavior as predicted by the short- and full-range models. Finally, we close with a summary of our findings and the future outlook.

TABLE 1: Lennard-Jones Parameters, ϵ_i and σ_i, Partial Charges q_i, Geometries of the Used Potential Models, and Their Resulting Dipole Moments

atom	ϵ/k_B (K)	σ (Å)	q (e)	geometry	μ (D)
			Acetonitrile[19]		
CH_3	104.15	3.775	+0.15	C−CH_3: 1.458 Å	3.44
C	75.53	3.650	+0.28	C−N: 1.157 Å	
N	85.54	3.200	−0.43	CH_3−C−N: 180°	
			Hydrogen Fluoride[17]		
F	75.76	2.984	+0.725	F−X: 0.166 Å	2.03
H	0.0	0.0	+0.725	F−H: 0.917 Å	
X	0.0	0.0	−1.45	F−X−H: 180°	
			Formic Acid[22]		
C	45.237	3.727	0.4447	C−$O_{(c)}$: 1.213 Å	1.22
$O_{(c)}$	146.06	2.674	−0.4324	C−$O_{(h)}$: 1.35 Å	
$O_{(h)}$	47.16	3.180	−0.5530	$O_{(h)}$−$H_{(a)}$: 0.98 Å	
$H_{(f)}$	2.406	0.80	0.1073	C−$H_{(f)}$: 1.096 Å	
$H_{(a)}$	12.03	0.994	0.4333	$O_{(c)}$−C−$O_{(h)}$: 125.1°	
				C−$O_{(h)}$−$H_{(a)}$: 106.1°	
				$O_{(c)}$−C−$H_{(f)}$: 125.1°	

TABLE 2: Parameters of the Switching Functions

	acetonitrile	hydrogen fluoride	formic acid
R_1, Å	6.5	5.25	6.0
R_2, Å	8.5	7.25	8.0

2. Basic Definitions and Computational Details

The considered realistic potentials are common site−site potentials that assume a rigid monomer with interaction sites located (but not necessarily) on the nuclei and generating two types of interactions: (1) neutral medium-range interaction with harsh short-range repulsions and medium-range dispersion, and (2) Coulombic sites with the zero net charge of the entire molecule. The interactions between two molecules are thus represented by the potential function of the form

$$u(1,2) \equiv u(R_{12},\Omega_1,\Omega_2) = \sum_{i\in\{1\}}\sum_{j\in\{2\}}\left\{4\epsilon_{ij}\left[\left(\frac{\sigma_{ij}}{r_{ij}}\right)^{12} - \left(\frac{\sigma_{ij}}{r_{ij}}\right)^{6}\right] + \frac{1}{4\pi\epsilon_0}\frac{q_i q_j}{r_{ij}}\right\} = u_{LJ}(1,2) + u_{coul}(1,2) \quad (1)$$

where the set (R_{12},Ω_i) defines, respectively, the mutual position (separation R_{12} between the reference sites) and orientation of a pair of molecules, r_{ij} denotes the separation between site i on molecule 1 and site j on molecule 2, $r_{ij} = |\mathbf{r}_1^{(i)} - \mathbf{r}_2^{(j)}|$, q_i are partial charges, and ϵ_{ij} and σ_{ij} are the Lennard-Jones (LJ) size and energy parameters, respectively. Specifically, for hydrogen fluoride we use the three-site OPLS model of Cournoyer and Jorgensen, referred to as the CJ84 potential,[17] because it gives a relatively adequate representation of the VLE in comparison to other available nonpolarizable models;[18] for acetonitrile we also use an OPLS model developed by Jorgensen and Briggs[19] that was already used in other studies[20,21] (though slightly modified with the use of the Lorentz−Berthelot rather than the original Lorentz combining rule); and for formic acid we use the model developed by Jedlovszki and Turi, and used in Gibbs ensemble simulations.[22] The geometry of all models are defined in Table 1 where the potential parameters and the resulting dipole moments are given as well.

For all models the geometric mean (i.e., Lorentz combining rule) is used not only for the energy to define the cross

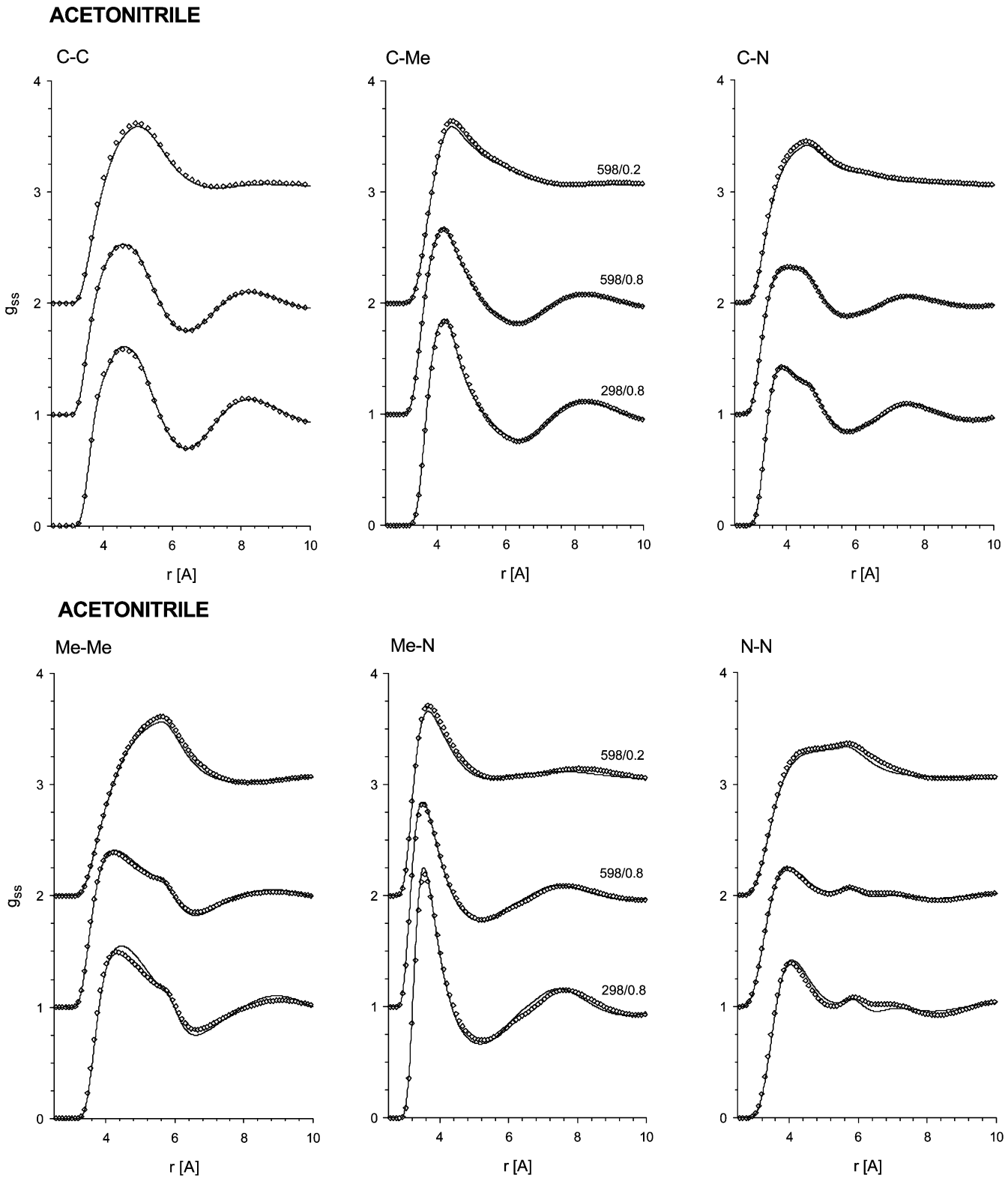

Figure 1. Site−site correlation functions of acetonitrile at the state points given by the tags [temperature/density] at the curves. The lines are the full potential model results and the symbols correspond to the short-range models; the functions are gradually shifted by 1.

interactions between the LJ sites of all compounds,

$$\epsilon_{ij} = (\epsilon_{ii}\epsilon_{jj})^{1/2} \tag{2}$$

but also for σ's,

$$\sigma_{ij} = (\sigma_{ii}\sigma_{jj})^{1/2} \tag{3}$$

To investigate the effect of the range of interactions on the structure of fluids, we construct a short-range potential, u_{sr}, by cutting off smoothly all the long-range interactions with respect to the reference sites,[5,7,23]

$$u_{sr}(1,2) = u(1,2) - S(R_{12};R_1,R_2)u_{coul}(1,2) = u_{LJ}(1,2) + [1 - S(R_{12};R_1,R_2)]u_{coul}(1,2)] \tag{4}$$

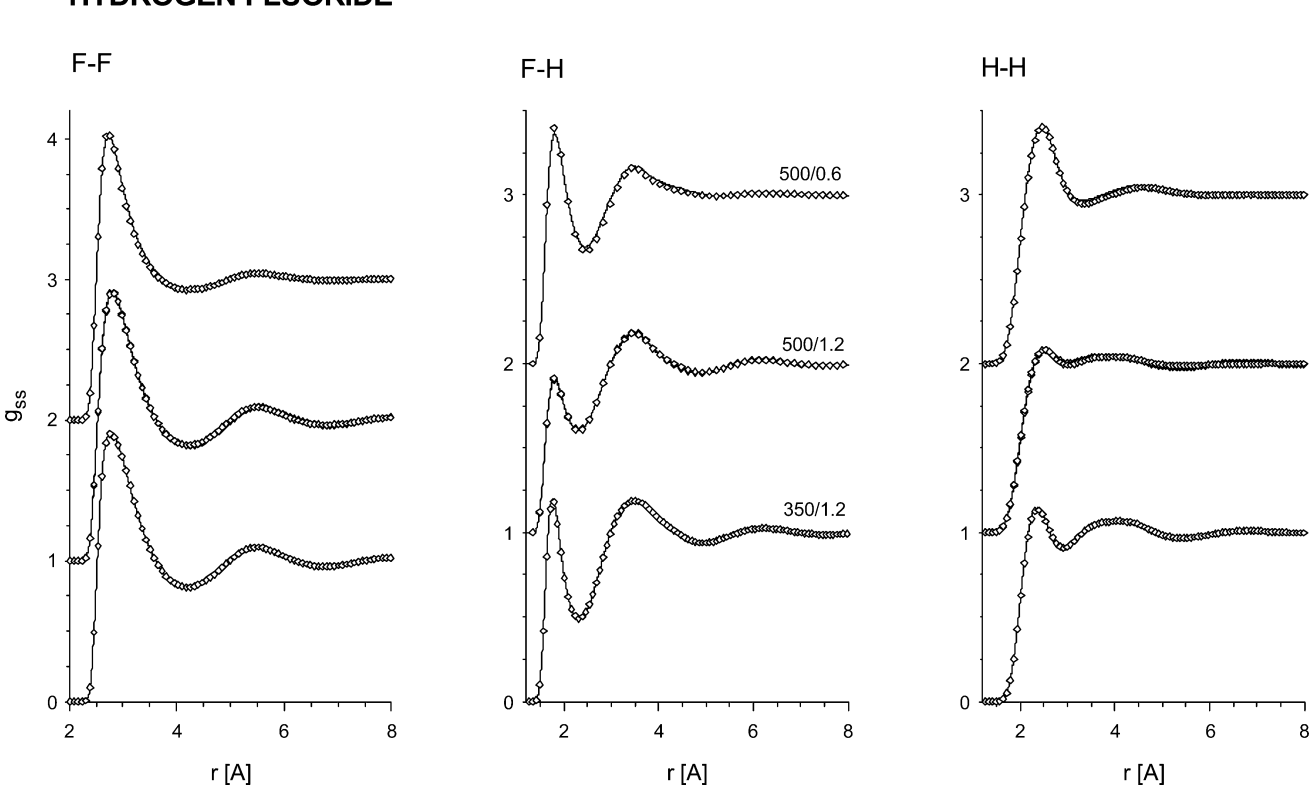

Figure 2. Same as Figure 1 for hydrogen fluoride.

where S is a switch function,

$$S(r;R_1,R_2) = \begin{cases} 0 & \text{for } r < R_1 \\ (r-R_1)^2(3R_2-R_1-2r)/(R_2-R_1)^3 & \text{for } R_1 < r < R_2, \\ 1 & \text{for r} > R_2 \end{cases} \quad (5)$$

where R_1 and R_2 are its parameters defining the transition range.

An alternative short-range model is also considered in this paper, namely, a theoretically appealing model suggested already long time ago[23] and briefly considered in our recent related study.[24] It makes use of the predominant dipole−dipole interaction at large separation and deducts only the dipole−dipole interaction instead of the entire Coulombic interaction,

$$u_{\text{sr, DD}}(1,2) = u(1,2) - S(R_{12};R_1,R_2)u_{\text{dipole - dipole}}(1,2) \quad (6)$$

Following the common practice we describe the structure of the fluid by the complete set of site−site correlation functions $g_{ij}(r_{ij})$ defined by

$$4\pi r_{ij}^2 g_{ij}(r_{ij}) = \left(1 - \frac{1}{N}\right) V \langle \delta(r_{ij} - |\mathbf{r}_1^{(i)} - \mathbf{r}_2^{(j)}|)\rangle \quad (7)$$

where the angular brackets denote an ensemble average. The axial orientational correlations are conveniently described by the multipole−multipole correlation functions $G_l(r)$ of order l (called also "local g-factors"[25]), $l = 1, 2$,

$$4\pi r^2 G_l(r) = \left(1 - \frac{1}{N}\right) V \langle \delta(r - |\mathbf{r}_1^{(i)} - \mathbf{r}_2^{(j)}|)\mathscr{P}_l(\cos\Theta_{12})\rangle \quad (8)$$

where $\mathscr{P}_l$ is the normalized Legendre polynomial, and Θ_{12} is the angle formed by the axes of molecules 1 and 2.

The natural quantity to measure in finite samples of a dipolar system is the fluctuation of the total dipole moment of the system, $\langle M^2\rangle$, which is related to the dielectric constant ϵ_r, where $M = \sum_{i=1}^{N}\mu_i$ and μ_i is the dipole moment of molecule i. Using the reaction field method[26] to treat the long-range Coulombic interactions and assuming the metal boundary conditions, the dielectric constant is evaluated as follows:

$$\frac{(\epsilon_r - 1)(2\epsilon_{rf} + 1)}{2\epsilon_{rf} + \epsilon_r} = \frac{\rho\mu^2 g_1}{3\epsilon_0 k_B T} \quad (9)$$

where

$$g_1 = \frac{\langle M^2\rangle}{N\mu^2} \quad (10)$$

is the Kirkwood g-factor (sometimes called "finite sample Kirkwood factor" to explicitly express its dependence on boundary conditions); it equals unity if the dipoles are uncorrelated.[27]

To study the systems away from the equilibrium orthobaric region (e.g., along a supercritical isochore and a supercritical isotherm), we ran molecular dynamics simulations with a total of 500 molecules at isothermal−isochoric conditions using a Nosé thermostat.[28] The Newton−Euler equations of motion were integrated using the fifth- and fourth-order Gears' predictor-corrector[29] for the translational and rotational degrees of freedom, respectively, with a time step of 1.0 fs. The rigid body orientations were described by the Evans−Murad quaternion formalism.[30] Similarly as in the previous paper,[8] long-ranged electrostatic interactions were handled by the reaction field method[26] with the metal-like boundary conditions, and the standard long-range corrections to pressure and the configurational internal energy due to nonelectrostatic interactions were

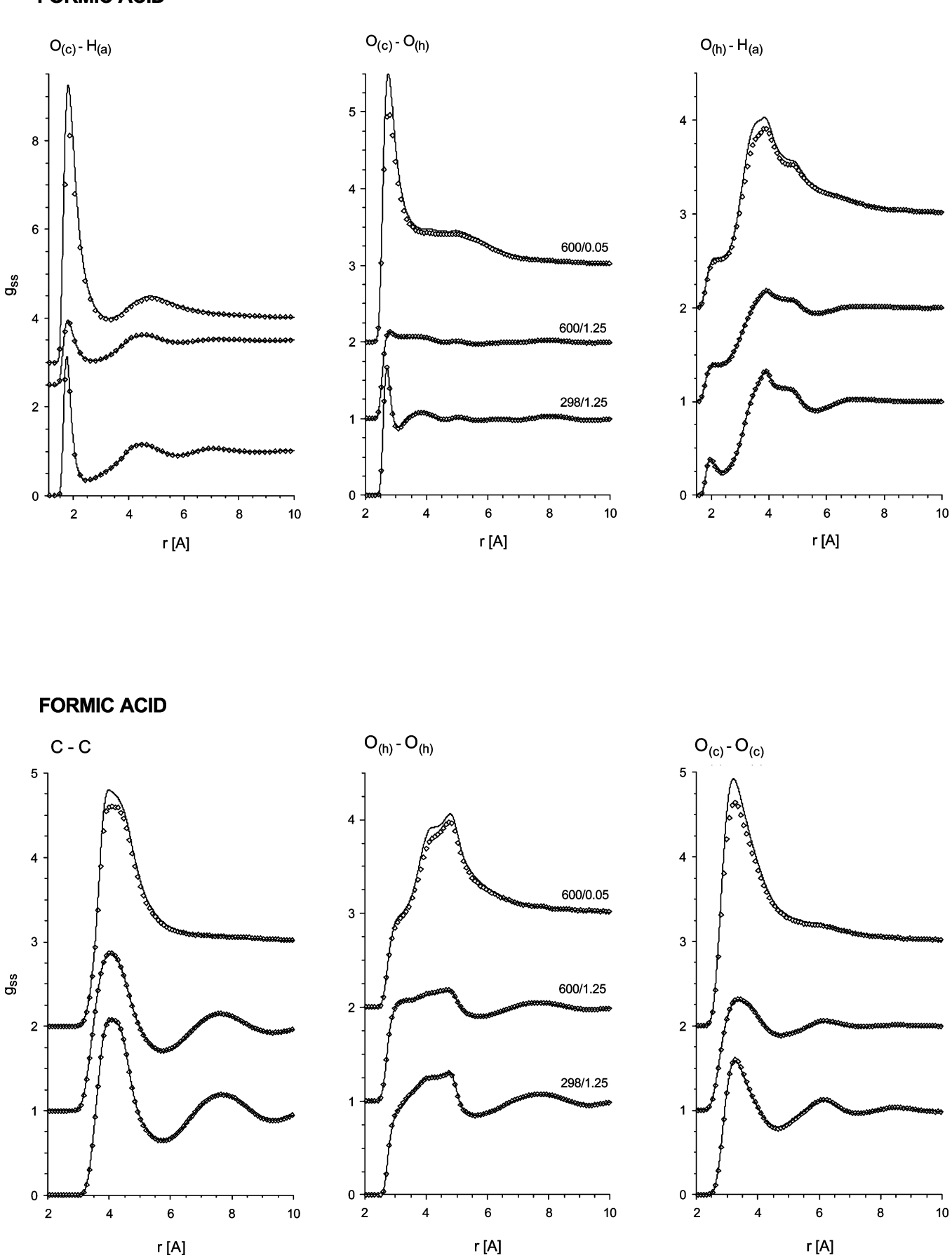

Figure 3. Same as Figure 1 for formic acid. The functions $O_{(c)}-H_{(a)}$ are shifted by 2.5 and 3, respectively, for clarity.

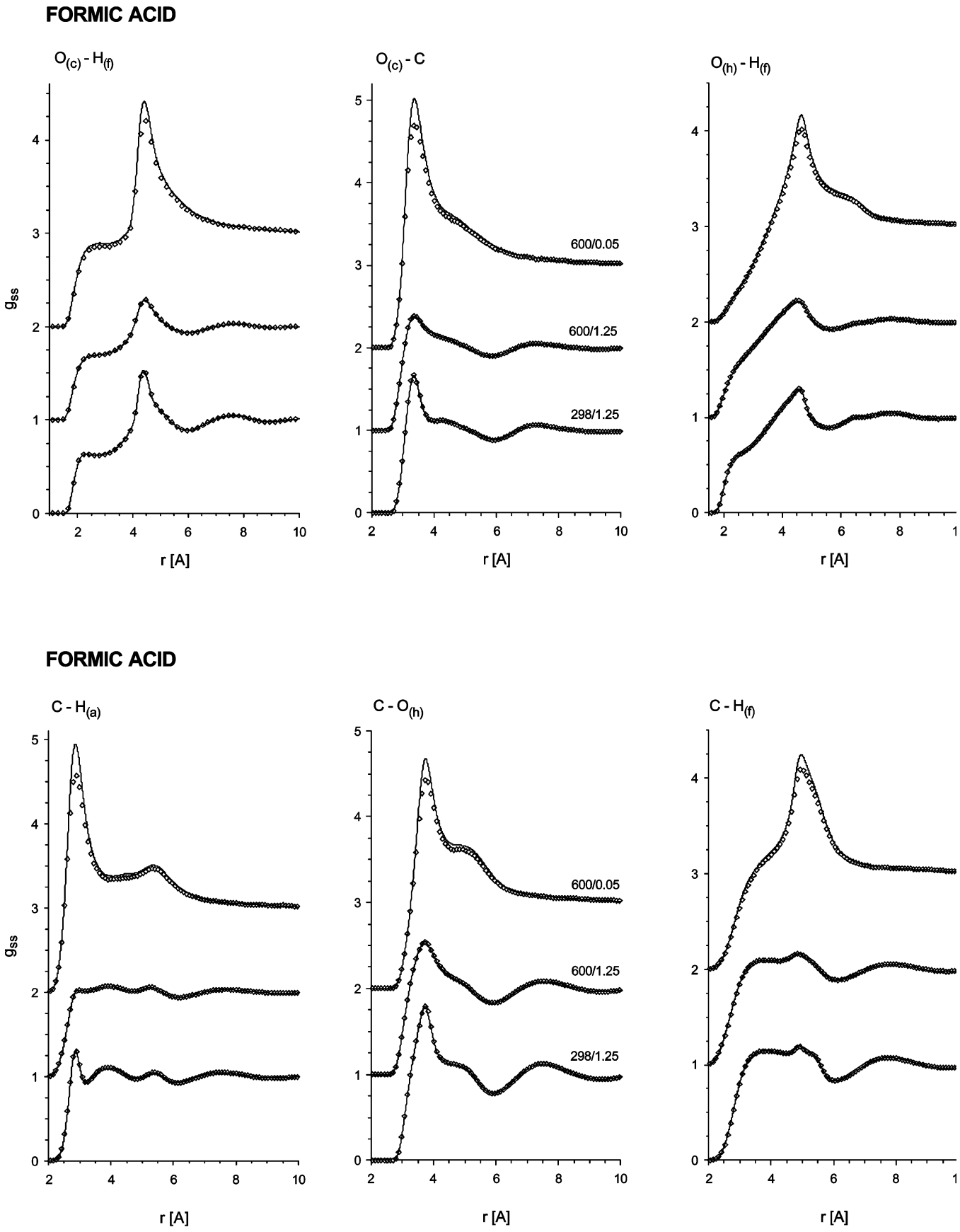

Figure 3. Continued.

added.[31] For that purpose all interactions were truncated at a cutoff distance $r_c = 3.5-4.0\sigma$ (where σ refers here to the Lennard-Jones size parameter of the reference sites), on the basis of the molecular center of mass to preserve electroneutrality.

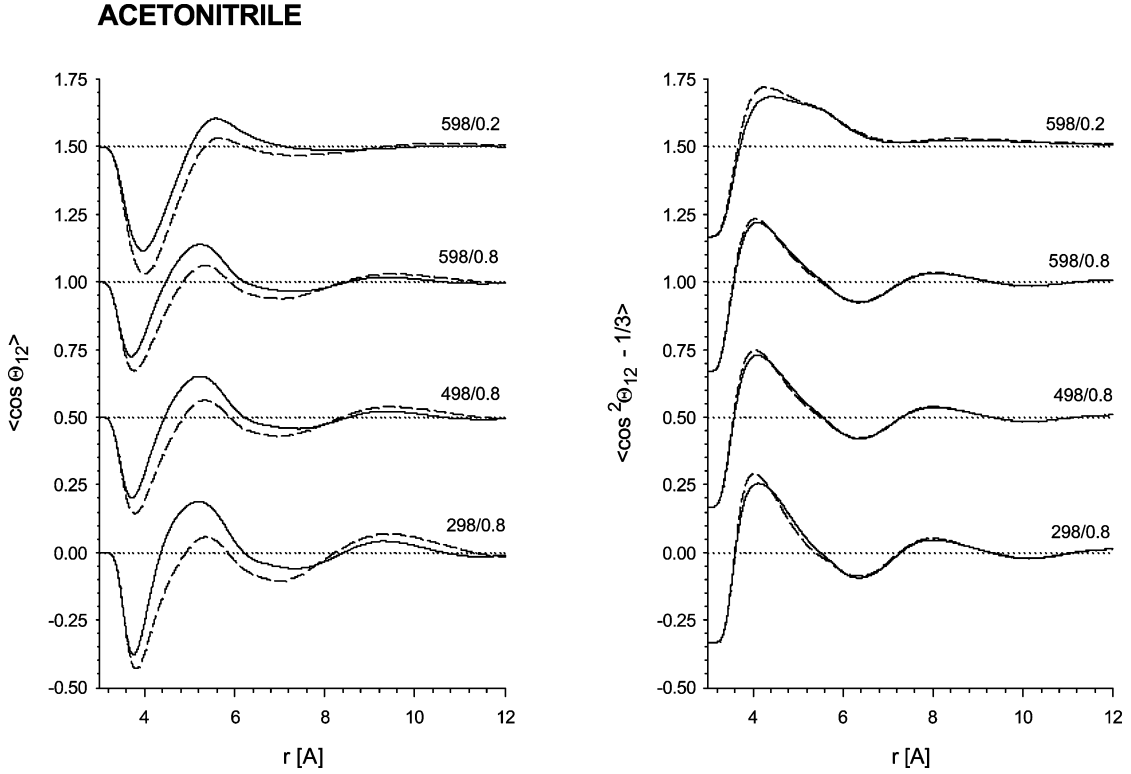

Figure 4. Unnormalized dipole−dipole correlation functions of the first (left) and second (right) order for acetonitrile at the state points given by the tags [temperature/density]. The solid lines are the full potential results, dashed lines correspond to the short-range models.

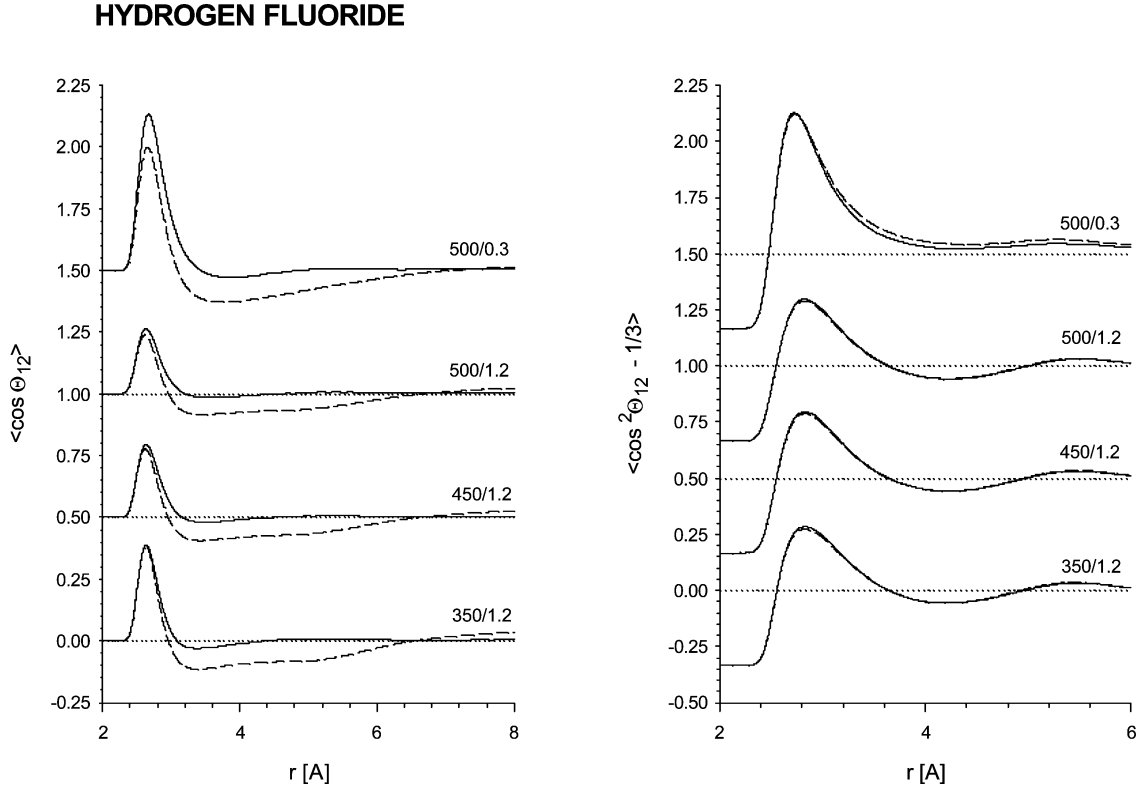

Figure 5. Same as Figure 4 for hydrogen fluoride.

Typical simulation runs spanned the interval of 200 ps following a 30 ps equilibration period. To assess the uncertainties of the simulation averages, the full run was divided into 20 subruns from which the quoted statistics were evaluated.[32] At selected thermodynamic states for which we calculated also the dielectric constant, the simulation runs covered 1.5 ns of the phase space trajectory.

For the vapor−liquid-phase equilibria calculations we ran standard NVT Gibbs Ensemble Monte Carlo simulations.[31,33] With the exception of the highest temperature, for which we used 600−700 particles, simulations at all other conditions were carried out with $N = 512$ particles, and the reaction field was used again to account for the long-range interactions. The number of particles in the vapor phase varied between 50 and

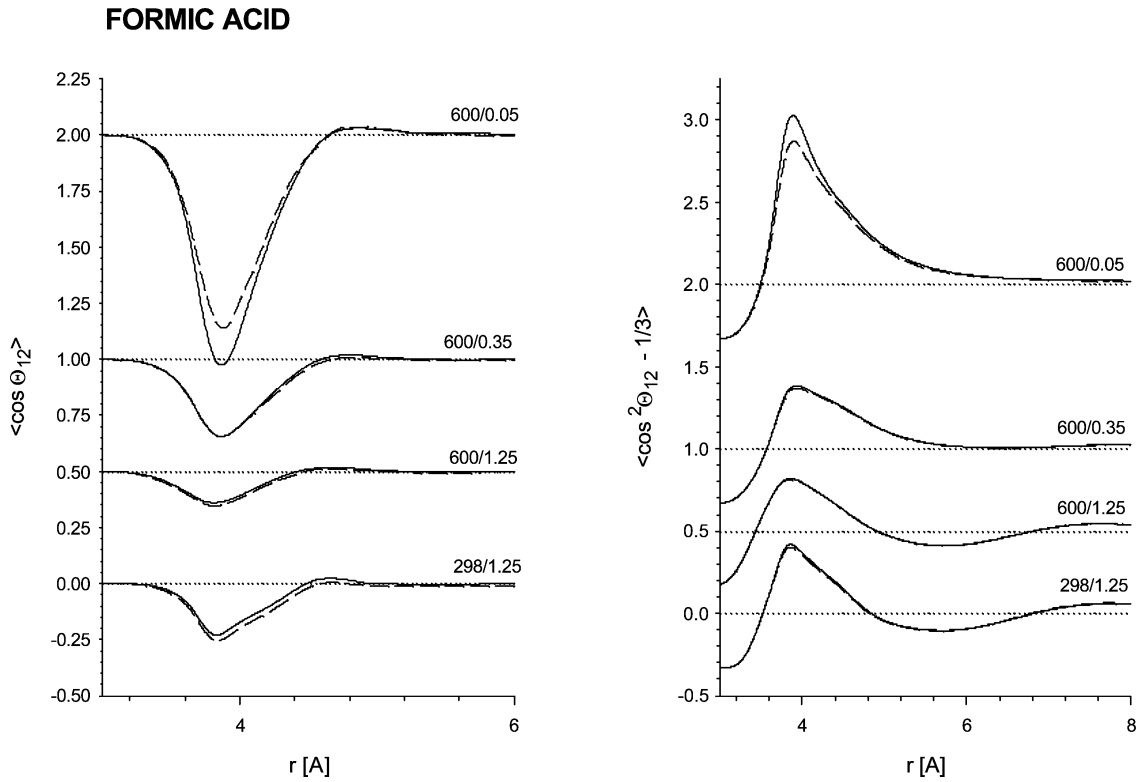

Figure 6. Same as Figure 4 for formic acid.

150 over the entire temperature range. The acceptance ratio for the trial moves was adjusted to about 1:2.

3. Results and Discussion

Following the approach used in our previous work,[8] we carried out two sets of simulations for each compound, i.e., one along a liquidlike isochore and the other along a supercritical isotherm, to assess the temperature and density dependence of the long-range contributions of the intermolecular forces to the system properties. In particular, for acetonitrile we analyzed the fluid behavior along the 0.8 g/cm^3 isochore within the temperature range 298−598 K, and then along the 598 K isotherm within the density range 0.2−0.8 g/cm^3. Likewise, for HF, these ranges were 350−500 K along the 1.2 g/cm^3 isochore, and 0.1−0.9 g/cm^3 along the 500 K isotherm. Finally, for formic acid the analysis covered the range 298−600 K along the 1.25 g/cm^3 isochore and 0.05−1.25 g/cm^3 along the 600 K isotherm. For each system we characterized the fluid behavior in terms of the configurational internal energy, the pressure, and all possible site−site pair distribution functions to determine the range of pair distances where the intermolecular potentials contribute the most ($r < R_2$ in our notation). Moreover, we also determined suitable values for the switching parameters R_1 and R_2 in eqs 4−6, according to the methodology developed previously.[6] These values, given in Table 2, are usually within the range up to (or slightly beyond) the first minimum of the radial distribution function for the site−site interaction taken as the center of the switching function, i.e., the F-site in hydrogen fluoride and the C-sites in formic acid and acetonitrile.

3.1. Structural and Thermodynamic Properties of the Homogeneous Phases. Because we are dealing with nonpolarizable intermolecular potential models, the model (effective) dipole moments are typically slightly different from the experimental ones, the result of accounting for polarization effects through augmented electrostatic charges (see Table 1). In fact, according to the tabulation of Gray and Gubbins,[3] the CJ84 model overpredicts the total dipole moment of HF by 7%,

TABLE 3: Predicted Dielectric Constant for the Full and Short-Range Models of Acetonitrile

	298 K 0.8 g/cm^3	598 K 0.8 g/cm^3	598 K 0.2 g/cm^3
full	18.1 ± 1	10.2 ± 0.4	2.7 ± 0.1
short-range	19.2 ± 2	10.5 ± 0.5	2.8 ± 0.1

whereas the Jorgensen−Briggs[19] and Jedlovszky−Turi[22] models underpredict the actual dipole moments of acetonitrile and formic acid by 19% and 15%, respectively.

In Figures 1−3 we show the behavior of the site−site pair distribution functions as predicted by the full and short-range potentials for the three fluids at some representative state conditions. The obvious feature in this comparison is that the distribution functions of the short-range potentials, according to the chosen switching range (Table 2), are practically indistinguishable from the corresponding full-range counterparts, perhaps with the exception of formic acid whose first peaks exhibit relatively small differences at high temperatures and very low densities. This is what we have already found for other types of model fluids, including water, carbon dioxide, methanol, and acetone,[8] though it does not provide any explicit information regarding differences in orientational behavior. Because the site−site radial distribution functions are, by definition, orientationally averaged properties, the source of the small differences found in the comparison of Figures 1−3 must be associated with differences in the orientational behavior of the two systems. For that reason we turn our attention to the predicted first and second-order dipole−dipole correlations as shown in Figures 4−6. Acetonitrile and formic acid, having both larger dipoles than HF, exhibit negative dipolar correlation at short distances; i.e., the first neighboring dipoles align in antiparallel configurations. The notable difference between these two dipole correlations is that the ordering disappears beyond the first coordination shell of formic acid, and attenuates in an oscillatory fashion for acetonitrile. In contrast, HF shows a positive dipole correlation for the first neighboring pairs, i.e., forming parallel

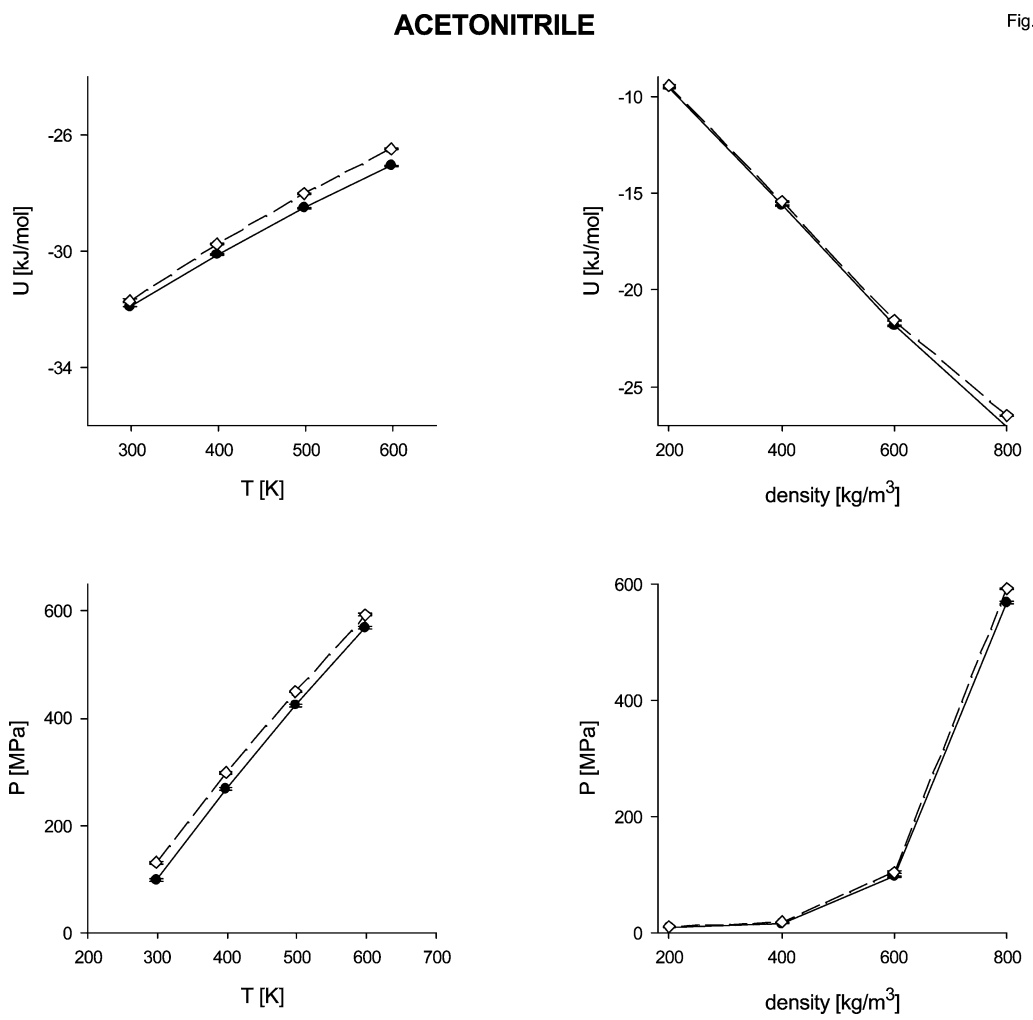

Figure 7. Internal energy and pressure of acetonitrile along high-density isochore (left column) and supercritical isotherm (right column). Filled circles are the results for the full potential model and the symbols correspond to the short-range model. The lines have been drawn as a guide for the eyes.

TABLE 4: Location of the Critical Point of the Short-Range and Full Models, and Their Effective Critical Exponents As Estimated from the Wegner Expansion, Eq 12

	short-range			full		
	T_c	ρ_c	β_e	T_c	ρ_c	β_e
acetonitrile	548.1	180.0	0.30	538.9	179.4	0.31
hydrogen fluoride	403.9	371.5	0.28	404.6	329.4	0.33
formic acid	543.0	415.9	0.29	540.2	422.5	0.27

dipole configurations, though this correlation dies out very quickly. Most important is the fact that, despite the observed small differences between the dipole−dipole correlations of the short and full range models, the corresponding dielectric constants are actually the same within the uncertainties of the simulation results, as indicated in Table 3 for acetonitrile. Noting that the dielectric constant is a measure of the volume integrals over the first-order dipole−dipole correlation function, our results confirm previous findings[7] indicating that the relatively small long-range effects on the orientational correlation functions have a minuscule impact into the predicted dielectric constant, even for this extreme dipolar system.

The thermodynamic properties for the three fluids, predicted by the short and full range interaction models, are compared in Figures 7−9. According to Figure 7 the long-range contributions to the properties of acetonitrile are negative for the internal energy as well as for the pressure along the 0.8 g/cm^3 isochore within the considered temperature range. The largest long-range contributions along the isochore are less than 2.5% and 25% for the internal energy and pressure, respectively. This behavior is also found for the high-temperature density dependence, though the differences become smaller with decreasing density as already seen in HF.

Note that, in contrast to acetonitrile, Figure 8 indicates that the long-range contributions to the properties of HF are positive for the internal energy and negative for the pressure along the 1.2 g/cm^3 isochore within the studied temperature range. The largest long-range contributions along the isochore are less than 1.2% and 10% for the internal energy and pressure, respectively. These differences become negligibly small with decreasing density along the 500 K isotherm.

Finally, the long-range contributions in formic acid are negative for both the internal energy and the pressure along the 1.25 g/cm^3 isochore within the temperature range (Figure 9), as found also for acetonitrile. The largest long-range contributions along the isochore are less than 1.0% and 1.5% for the internal energy and pressure, respectively. These differences become much smaller with decreasing density along the 600 K isotherm, as already found for the other cases.

The above findings are not unexpected considering that the impact of the long-range portion of the intermolecular potential on the system microstructure, Figures 1−3, is rather negligible. In fact, the largest effect is always observed on the pressure because the average virial of the system is more sensible to the

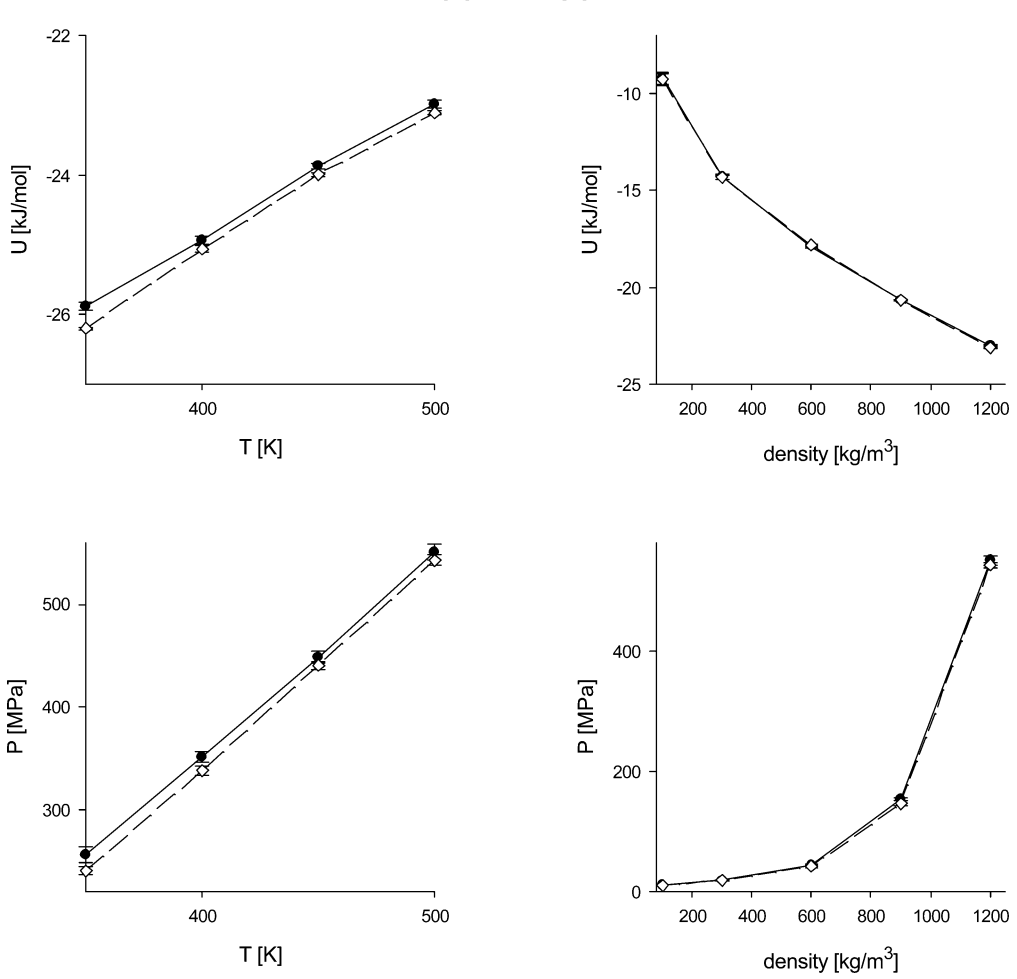

Figure 8. Same as Figure 7 for hydrogen fluoride.

details of the intermolecular potential (i.e., integral over the gradient of the potential) than the corresponding configurational energy (i.e., integral over the potential function itself). Moreover, the average virial usually exhibits stronger dependence on orientational correlations than the configurational energy, and according to Figures 4−6, the orientational correlations are more sensitive to the range of the interactions than the corresponding radial distribution functions.

Note, however, the temperature dependence of the second virial coefficient of the three models (left-hand-side ordinates in Figure 10), as determined explicitly by the 6-fold phase space integration based on a modified implementation of the Conroy's method.[34] The relative contributions of long-range interactions to the second virial coefficient of these models (right-hand-side ordinates in Figure 10) at the estimated critical temperature of the corresponding systems are approximately 0.5%, 0.8%, and 9% for HF, formic acid, and acetonitrile, respectively, whereas at twice the critical temperature these become 2.0%, 3.6%, and 16%, respectively. Moreover, note that these long-range contributions are negative, their magnitude goes as the total dipole moment of the model (i.e., the leading term in the multipole expansion of the electrostatic interactions, eq 6), and their absolute values decrease monotonically with increasing temperature as we could have expected from the definition of B_2.

3.2. Vapor−Liquid Coexistence Properties and Estimated Critical Conditons. In Figures 11−16 we compare the density, internal energy and pressure for the vapor−liquid equilibrium of the short and full range potentials for the three compounds. Note that in this comparison we include the predictions of the two alternative definitions for the short-range potential, i.e., eqs 4 and 6. In contrast to all the other systems previously studied, acetonitrile (having the largest dipole moment of all) exhibits a distinct behavior, in that the orthobaric densities for the full potential are larger than the corresponding short-range counterparts for the same equilibrium temperature, though at $T =$ 400 K, there is a clear inversion of this behavior in the liquid branch. For the vapor branch, the full potential predicts always a similar or larger orthobaric density than the corresponding short-range potential at the equilibrium temperatures. In contrast, the internal energies for the liquid branch are always larger (less negative) for the full potential than for the short-range counterparts, whereas the opposite is true for the vapor branch of the coexistence envelope (see Figures 11 and 14).

Following with HF we note that, as per the case of its behavior along the isolines above, the long-range part of the potential exhibits a positive contribution to the internal energy along the liquid branch of the envelope, but a negligible contribution to the vapor branch, except for $T <$ 300 K, where the internal energy of the full potential becomes more negative than the short-range counterpart. Note that the prediction of the vapor pressure for the short and full range potential is within the simulation uncertainties, though there is a clear negative contribution by the long-range intermolecular forces for $T >$ 350 K. In addition, the short-range potential predicts a denser liquid phase than that for the full range model at the same

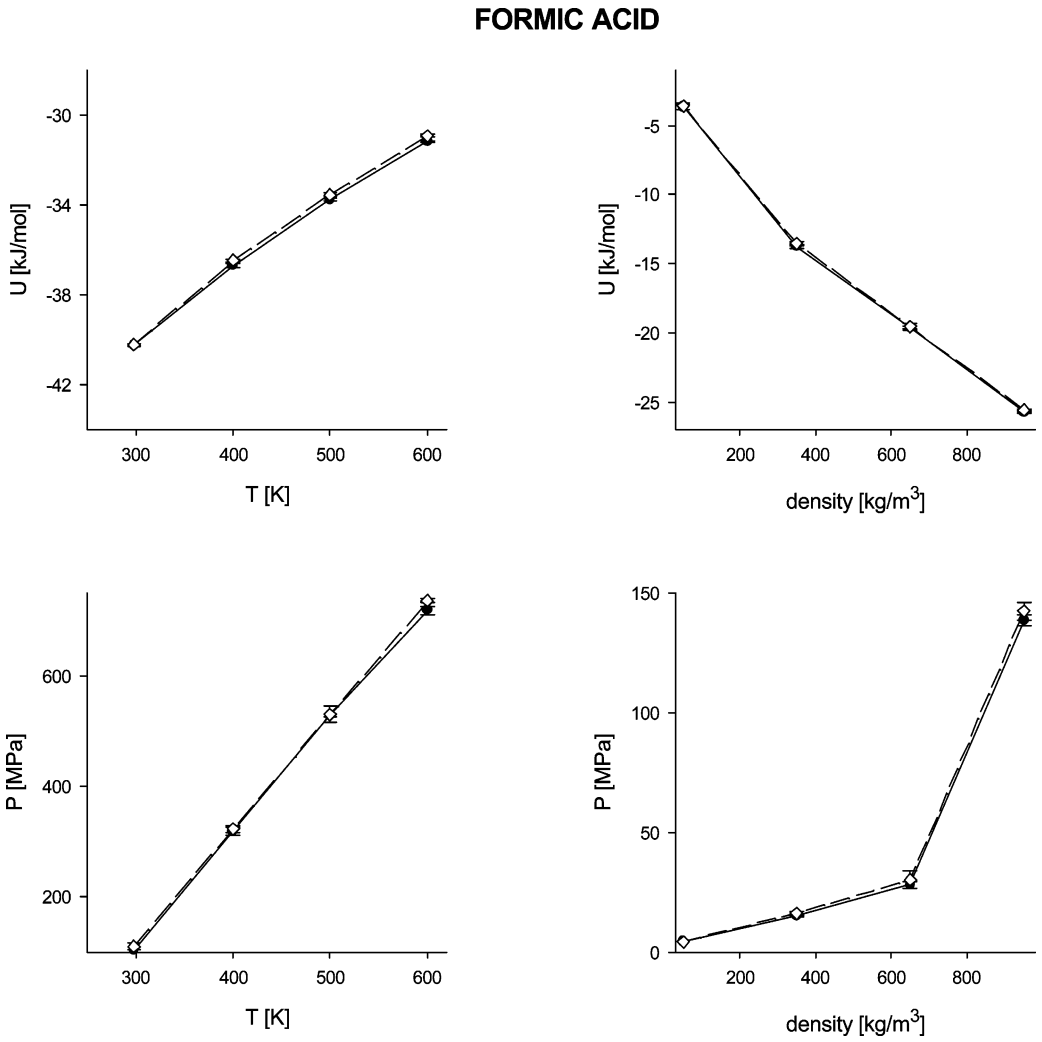

Figure 9. Same as Figure 7 for formic acid.

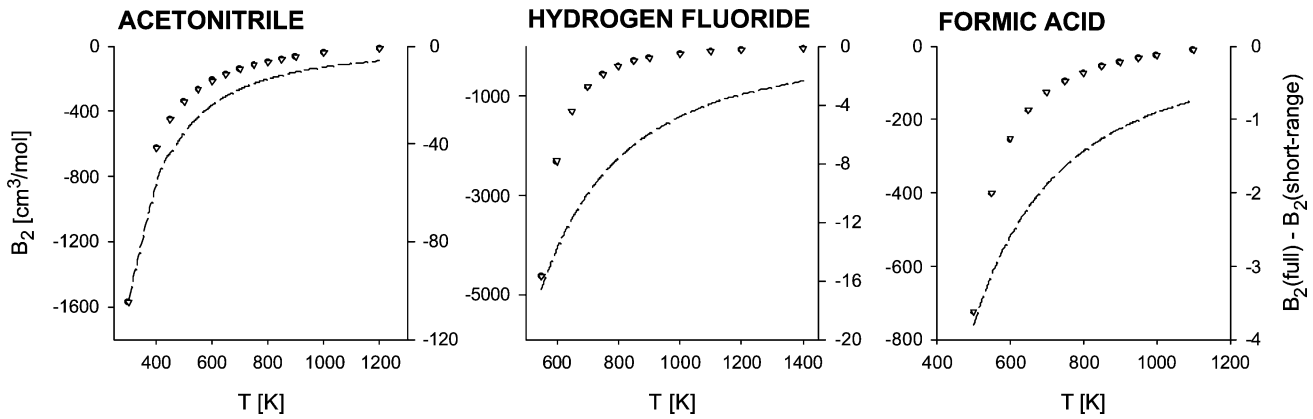

Figure 10. Comparison of the second virial coefficients of the full (filled symbols) and short-range (open symbols) models, and their difference (dashed line).

equilibrium temperature, whereas for the vapor branch the difference in orthobaric densities is negligibly small. By comparing these findings with those corresponding to water (see Figures 6−7 of ref 6), we can confirm that the long-range intermolecular forces contributions to the coexistence properties of HF behave (not surprising) similarly to those of water. The only noticeable difference is in the low temperature region of the phase envelope, where possible clustering/dimerization may occur in the vapor phase (see Figures 12 and 15). Note, however, that this effect is not clearly manifested for the case of the alternative short-range model.

Formic acid exhibits features already seen in the behavior of HF, such as the change in the trend of the temperature dependence of the internal configurational energy for the vapor branch of the coexistence envelope, and in CO2 [8], where the coexistent densities for the full system are slightly larger (smaller) in the liquid (vapor) phase, resulting in a slightly lower vapor pressure than that corresponding to the short-range counterpart (see Figures 13 and 16).

From a strictly modeling viewpoint the relevant question to be answered is: What is the net effect of the potential range on the location of the critical point? For that purpose we invoke

ACETONITRILE

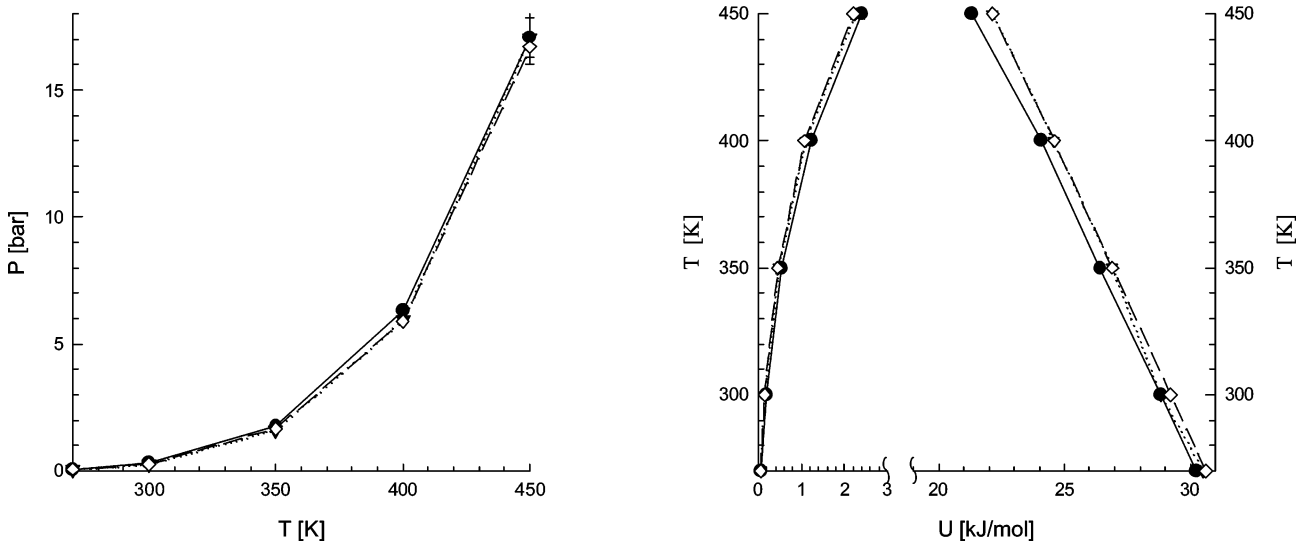

Figure 11. Internal energy and pressure of acetonitrile along the vapor−liquid coexistence curve. Filled circles are the results for the full potential model, open diamonds correspond to the short-range model obtained by switching off the long-range Coulombic part, eq 4, and filled triangles correspond to an approximate short-range model obtained by deducting the dipole−dipole interaction, eq 6. The corresponding lines (solid, dashed, dotted) have been drawn as a guide for the eyes.

HYDROGEN FLUORIDE

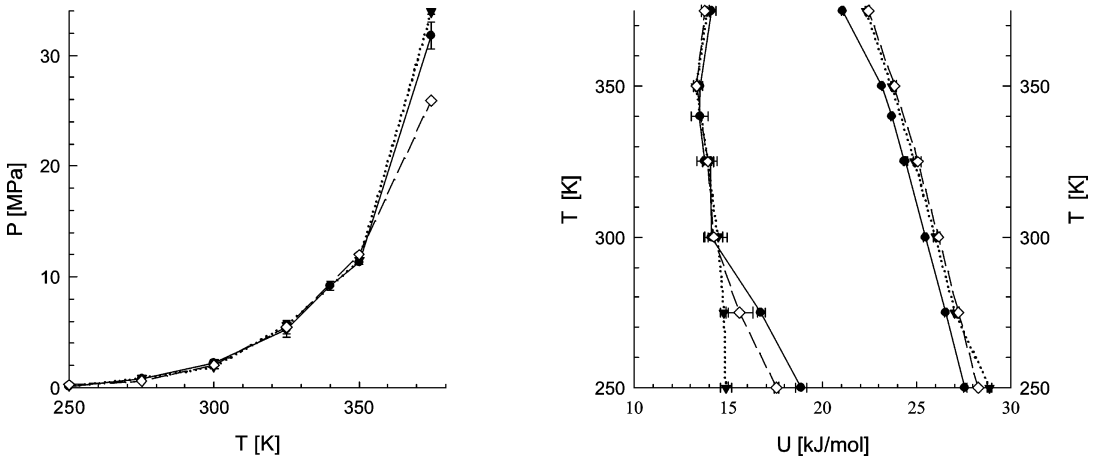

Figure 12. Same as Figure 11 for hydrogen fluoride.

the Wegner expansion for the coexistence envelope around the critical point[35]

$$\rho_l - \rho_v = A_0\Delta T^{\beta} + A_1\Delta T^{\beta+\Delta} + A_2\Delta T^{\beta+2\Delta} + ... \quad (11)$$

where $\Delta T = |\ 1 - T/T_c|$, T_c is the critical temperature, A_i are the amplitude coefficients, β is the critical exponent, and Δ is the so-called gap exponent. This equation can be used to estimate, by regression of experimental data, the critical temperature and the exponent β. Moreover, for the estimation of the corresponding critical density, ρ_c, we invoke the truncated equation for the rectilinear coexistence diameter (for details see, e.g., refs 36 and 37), i.e.,

$$\frac{\rho_l + \rho_g}{2} = \rho_c + B_2\Delta T \pm \frac{1}{2}A_0\Delta T^{\beta_e} \quad (12)$$

Following the common practice (see, e.g., refs 36 and 37), the coefficients B_1 and B_3, A_1, and higher order coefficients are set to zero, which yields the working equation

$$\rho\pm = \rho_c + B_2\Delta T \pm \frac{1}{2}A_0\Delta T^{\beta_e} \quad (13)$$

where the subscript e at β indicates that the exponent is considered as an effective quantity. To evaluate simultaneously determination the critical density, the critical temperature, and the effective critical exponent, we apply a least-squares method whose resulting values are given in Table 4. These results indicate that the long-range contributions to the intermolecular interactions have practically no effect on the values of the critical conditions, and confirm our previous findings[8] even for molecular systems characterized by increasingly larger dipole moments and/or stronger association.

3.3. Discussion and Final Remarks. It is a common modeling practice to add all relevant contributions to the full

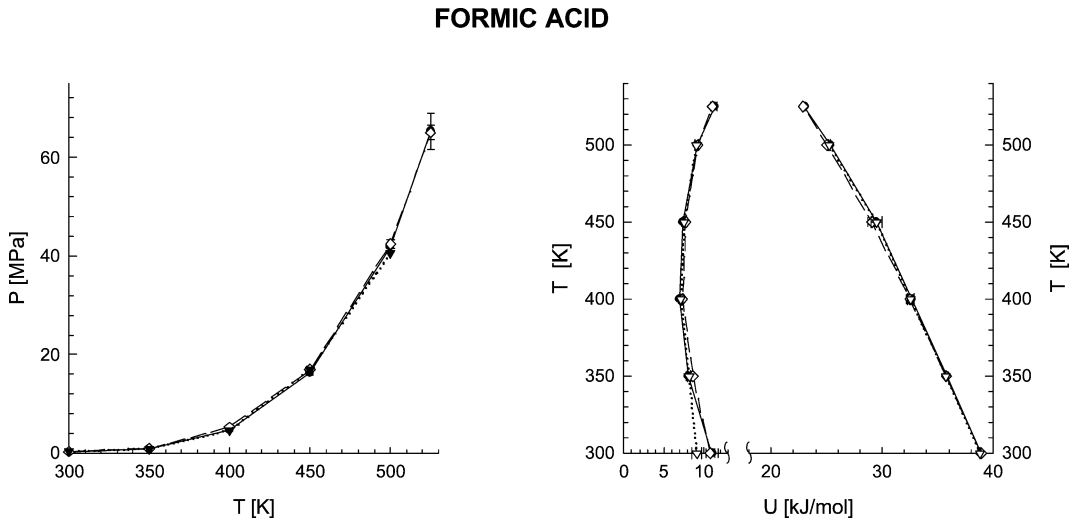

Figure 13. Same as Figure 11 for formic acid.

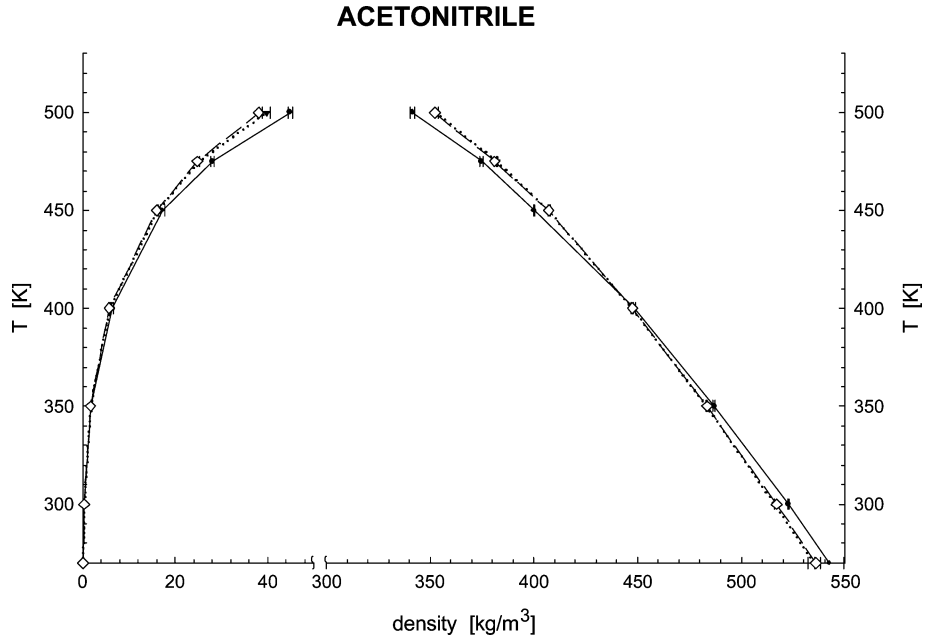

Figure 14. Vapor−liquid coexisting densities of acetonitrile. For symbols and lines see the caption for Figure 11.

effective pair interaction potential to capture more faithfully the thermodynamic behavior of a fluid.[38] Usually, this is achieved by starting with a dispersion contribution (Lennard-Jones and/or alike) to which additional terms are added, including electrostatic, association, and hydrogen bonding, according to the type of fluid under consideration. Although this approach can potentially make the modeling process flexible enough, and even very successful, for correlation purposes, it can also become rather misleading in that their flexibility and success might be the result of pure and fortuitous cancellation of errors/misrepresentations from each individual portion of the effective potential. In fact, it has long been demonstrated that, even for simple fluids such as atomic and polyatomic nonCoulombic fluids,[10] their thermodynamic properties depend almost exclusively on some attribute of the *full* effective potential rather than on individual components, the ones that ultimately govern the microstructure of the fluid. Just as per the case of simple fluids, and regardless of its nature, the relevant attribute of the full potential appears to be its range.[4]

To test this idea and unravel its connection with the resulting microstructure as well as with the corresponding thermodynamic behavior, we played with the range of the effective potential by introducing a radial function that switches off smoothly the electrostatic interactions, usually after the first solvation shell of the reference site. Alternatively, the short-range potential is obtained by subtracting the leading multipole−mutipole (e.g., the dipole−dipole in the case of dipolar fluids) interactions from the full pair interaction potential.

Although these artificial potential range-shortenings appear to affect only marginally the structure of the first nearest neighbors (i.e., represented by the corresponding site−site radial distribution functions), the impact on orientational distributions (i.e., described by the dipole−dipole correlations) is more pronounced. Yet, the corresponding integral over the first-order dipole−dipole correlation appears to effectively attenuate these differences to the point that the resulting dielectric constants exhibit a negligibly small dependence on the range of the pair potential.

The present results for these polar systems support our earlier assertion that the structure of pure fluids, as described by the corresponding site−site pair distribution functions, involving polar and associating interactions can be ascribed to the same

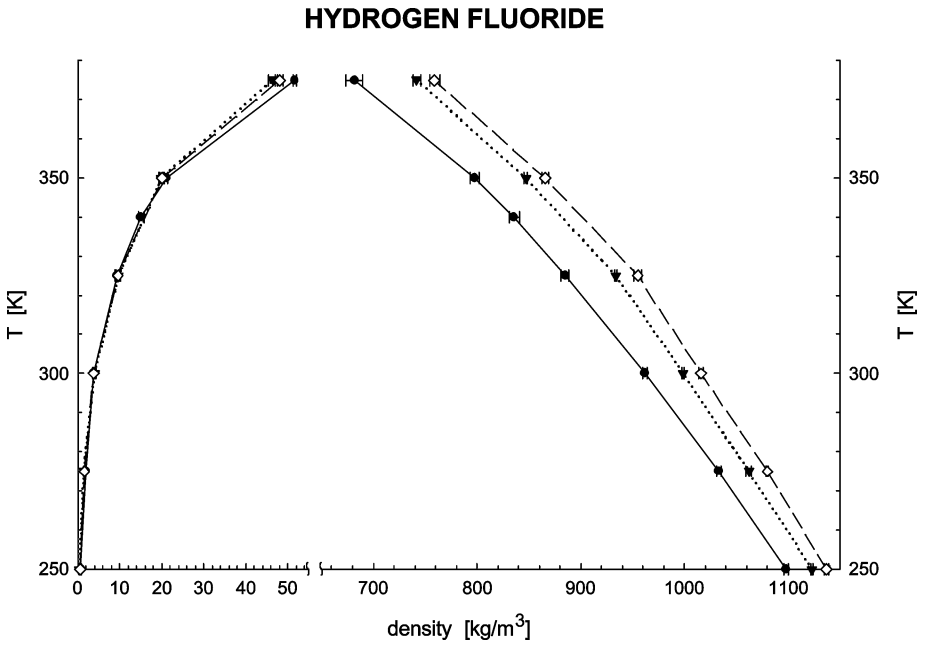

Figure 15. Same as Figure 14 for hydrogen fluoride.

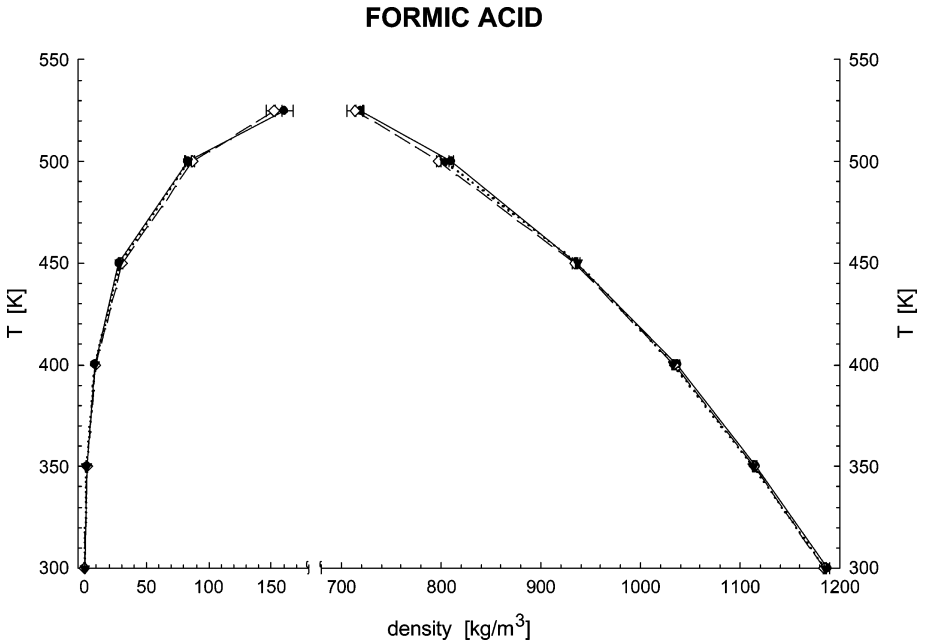

Figure 16. Same as Figure 14 for formic acid.

mechanism as for simpler fluids (e.g., systems with nonelectrostatic interactions), whereas the long-range portion of the electrostatic interactions (regardless of their strength) contributes only marginally. This behavior paves the way for a convenient perturbation expansion approach to the description of the thermophysical properties of highly polar/associative systems, about the reference described by the corresponding short-range potential counterpart (according to either eq 4 or 6), so that the long-range electrostatic contributions can be safely considered and evaluated as a perturbation about the reference system. In fact, the viability of this zeroth-order approximation has been successfully illustrated for the first time by the development of a truly molecular-based equation of state for water with accuracy similar to that of the available multiparameter correlation-based ones.[12]

The key to an accomplishment of a perturbation expansion, in general, is the ability to describe theoretically the properties of the short-range reference system. This may be achieved by mapping the properties of such a reference onto the properties of a suitable simple (primitive) model. As a well-known example of such a suitable model is the model of hard spheres that serves this purpose for simple (Lennard-Jones-like) fluids. The stumbling block in this endeavor for polar and associating fluids is to establish a similar adequate simple model that (i) captures the essential physics and (ii) simultaneously becomes theoretically tractable. This task has been traditionally tackled by using a large dose of intuition and/or inspiration. However, we have recently developed a more fundamental approach to build the primitive counterpart of a realistic intermolecular potential for associating[13−15] and polar[16] fluids as their direct descendant. The resulting short-range primitive model, composed of fused-hard-sphere bodies with embedded square-well attractive and hard-sphere repulsive sites mimicking the short-range electrostatic interactions, reproduces accurately the complete set of

the site−site radial distribution functions describing the fluid microstructure. Furthermore, a variant of the second-order thermodynamic perturbation theory has been developed to estimate accurately its properties[39] and thus the model properties can be obtained in a consistent manner. Developing a theory of complex fluids along this path seems therefore a likely and natural further continuation of the present work.

Acknowledgment. This research was supported by the Grant Agency of the Academy of Sciences of the Czech Republic (Grant No. IAA4072303), and by the Division of Chemical Sciences, Geosciences, and Biosciences, Office of Basic Energy Sciences, under contract DE-AC05-00OR22725 with Oak Ridge National Laboratory, managed by UT-Battelle, LLC.

References and Notes

(1) Rowlinson, J. S.; Swinton, F. L. *Liquids and Liquid Mixtures*; Butterworth: London, 1982.
(2) Reed, T. M.; Gubbins, K. E. *Applied Statistical Mechanics*; Butterworth-Heinemann: Stoneham, U.K., 1991.
(3) Gray, C. G.; Gubbins, K. E. *Theory of Molecular Fluids*; Clarendon Press: Oxford, U.K., 1984.
(4) Nezbeda, I. *Mol. Phys.* **2005**, *103*, 59−76.
(5) Nezbeda, I.; Kolafa, J. *Mol. Phys.* **1999**, *97*, 1105−1116.
(6) Kolafa, J.; Nezbeda, I. *Mol. Phys.* **2000**, *98*, 1505−1520.
(7) Kolafa, J.; Nezbeda, I.; Lísal, M. *Mol. Phys.* **2001**, *99*, 1751−1764.
(8) Kettler, M.; Nezbeda, I.; Chialvo, A. A.; Cummings, P. T. *J. Phys. Chem. B* **2002**, *106*, 7537−7546.
(9) Barker, J. A.; Henderson, D. *Rev. Mod. Phys.* **1976**, *48*, 587−671.
(10) Weeks, J. D.; Chandler, D.; Andersen, H. C. *J. Chem. Phys.* **1971** *54*, 5237−5247. Fischer, J.; Lago, S. *J. Chem. Phys.* **1983**,*78*, 5750−5758.
(11) Nezbeda, I. *Fluid Phase Equilib.* **2001**, *182*, 3−15.
(12) Nezbeda, I.; Weingerl, U. *Mol. Phys.* **2001**, *99*, 1595−1606.
(13) Nezbeda, I.; Vlček, L. *Int. J. Thermophys.* **2004**, *25*, 1037−1049.
(14) Vlček, L.; Nezbeda, I. *Mol. Phys.* **2003**, *101*, 2987−2996.
(15) Vlček, L.; Nezbeda, I. *Mol. Phys.* **2004**, *102*, 485−497.
(16) Vlček, L.; Nezbeda, I. *Mol. Phys.*, in press.
(17) Cournoyer, M. E.; Jorgensen, W. L. *Mol. Phys.* **1984**, *51*, 119−132.
(18) Visco, D. P.; Kofke, D. A. *J. Chem. Phys.* **1998**, *109*, 4015−4027; *Fluid Phase Equilib.* **1999**, *160*, 37−47.
(19) Jorgensen, W. L.; Briggs, J. M. *Mol. Phys.* **1988**, *63*547−558.
(20) Mountain, R. D. *J. Chem. Phys.* **1997**, *107*, 3921−3923.
(21) Guardia, E.; Pinzon, R.; Casulleras, J.; Orozco, M.; Luque, F. J. *Mol. Simul.* **2001**, *26*, 287−306.
(22) Jedlovszky, P.; Turi, L. *J. Phys. Chem. A* **1997**, *101*, 2662−2665; *J. Phys. Chem. A* **1999**, *103*, 3796−3796.
(23) Nezbeda, I.; Kolafa, J. *Czech. J. Phys. B* **1990**, *40*, 138−150.
(24) Nezbeda, I.; Lísal, M. *Mol. Phys.* **2001**, *99*, 291−300.
(25) Steinhauser, O. *Mol. Phys.* **1982**, *45*, 335−348.
(26) Neumann, M. *Mol. Phys.* **1983**, *50*, 841−853.
(27) Kirkwood, J. G. *J. Chem. Phys.* **1939**, *7*, 911−919.
(28) Nosé, S. *Mol. Phys.* **1984**, *52*, 255−268.
(29) Gear, C. W. *The Numerical Integration of Ordinary Differential Equations of Various Orders*; Argonne National Laboratory: Chicago, 1966.
(30) Evans, D. J.; Murad, S. *Mol. Phys.* **1977**, *34*, 327−331.
(31) Allen, M. P.; Tildesley, D. J. *Computer Simulation of Liquids*; Clarendon Press: Oxford, U.K., 1987.
(32) Flyvbjerg, H.; Petersen, H. G. *J. Chem. Phys.* **1989**, *91*, 461−466.
(33) Frenkel, D.; Smit, B. *Understanding Molecular Simulation: From Algorithms to Applications*; Academic Press: San Diego, CA, 1996.
(34) Nezbeda, I.; Kolafa, J.; Labík, S. *Czech. J. Phys. B* **1989**, *39*, 65−79.
(35) Wegner, F. J. *Phys. Rev.* **1972**, *B 5*, 4529−4536.
(36) Green D. G.; Jackson G.; Demiguel E.; Rull L. F. *J. Chem. Phys.* **1994**, *101*, 3190−3204.
(37) Vega, L.; Demiguel, E.; Rull, L. F.; Jackson, G.; McLure, I. A. *J. Chem. Phys.* **1992**, *96*, 2296−2305.
(38) Prausnitz, J. M.; Lichtenthaler, R. N.; de Azevedo, E. G. *Molecular Thermodynamics of Fluid Phase Equilibria*; Prentice Hall: Englewood Cliffs, NJ, 1986.
(39) Vlček, L.; Nezbeda, I. *Mol. Phys.* **2003**, *101*, 2921−2927.